Experimental Evaluation and Numerical Modeling of Catalytic Activity of Ag-Fe Nanoparticles Systems Prepared by Microwave Synthesis Method for CO Oxidation

A.A. Elzatahry[1,], Hassan M. Hassan[2], M. ELSayed Youssef [3,*]*

[1] Polymer Materials Research Department, Advanced Technology and New Materials Research Institute, Mubarak City, Egypt
[2] Department of Chemistry, Faculty of Science, Suez Canal University, Egypt
[3] Computer Based Engineering Applications Department, IRI, Mubarak city, Egypt
[*]E-mail: elsayed168@gmail.com, aelzatahry@mucsat.sci.eg

We report a synthesis of Ag-Fe Oxide nano powder catalyst prepared by Microwave synthesis method, which is very active for low-temperature CO oxidation. Using XRD and TEM characterization techniques, we elucidated the surface composition change during catalysis process. The XRD patterns show that particle size increased during the catalysis process as a result of particle growth due to temperature effect. The activity of the prepared catalysts was studied to obtain the effects of the catalyst composition, and the preparation method on CO oxidation at low temperature. In this paper we present a methodology for modelling of local reaction-transport processes in porous heterogeneous catalyst. The CO oxidation on a catalyst with an consideration of flow of the reactant gases over the catalyst surface, the distance between surface and flow layers have been employed in the model. The reaction takes place on the catalyst sites located on the surface and in its pores, simultaneously with the transport of gaseous reaction components. The proposed model shows the effect of mass transfer limitations on a catalytic reaction. it shows the concentration gradient through the catalyst surface and provides an explanation of low and high conversions as a factor of gas layers over catalyst surface.

1. INTRODUCTION

During typical daily activities, people encounter carbon monoxide in a variety of microenvironments — while traveling in motor vehicles, working at their jobs, visiting urban locations associated with combustion sources, or cooking and heating with domestic gas, charcoal or wood fires

— as well as in tobacco smoke. Overall, the most important carbon monoxide exposures for a majority of individuals occur in the vehicle and indoor microenvironments.

The health significance of carbon monoxide in ambient air is largely due to the fact that it forms a strong bond with the hemoglobin molecule, forming carboxyhaemoglobin, which impairs the oxygen carrying capacity of the blood. The dissociation of oxyhemoglobin in the tissues is also altered by the presence of carboxyhemoglobin, so that delivery of oxygen to tissues is reduced further. The affinity of human haemoglobin for carbon monoxide is roughly 240 times that for oxygen, and the proportions of carboxyhemoglobin and oxyhemoglobin formed in blood are dependent largely on the partial pressures of carbon monoxide and oxygen. Consequently, the development of low-temperature CO oxidation catalysts has received considerable attention. It remains a need for development of catalysts which exhibit higher activities for prolonged periods at low temperatures (typically less than 100 ^{o}C) and in the diverse range of oxidation environments which are encountered. Catalytic CO oxidation by silver supported on reducible metal oxides has been intensively studied by a number of investigators in recent years. Mn/Ag composite oxide of silver and manganese is a good CO oxidation catalyst, it also showed that the interaction between the manganese and silver resulted in a catalyst that was much more active than either component [1]. Also low loading silver manganese oxide catalysts and found them to be active low temperature CO oxidation[2] . The activities of $\sim$10% silver cobalt oxide catalysts in an excess of O_2, was tested to show an active low temperature catalyst[3]. Also it has been approved the presence two kinetically distinct atomic oxygen species exist on Ag, which exhibit a very high probability for the CO oxidation reaction[4, 5].

Conventional hydrothermal method is often substituted by the microwave assisted hydrothermal method because this method offers very rapid heating, faster kinetics, phase purity with better yield, homogeneity and high reproducibility. Only a few publications reported studies on microwave-assisted inorganic synthesis[6]. The synthesis of supported nanoparticle catalysts via microwave irradiation has been reported , showing the significance of this method, which lies mainly in its simplicity, flexibility, and the control of the different factors that determine the activity of the nanoparticle catalysts[7,8]. Nowadays, computer-aided catalyst design and optimisation of porous structures are of increasing importance in research and industry. Significant advances have been made in the development of models and methods for the simulation of reaction, transport and transformation processes in porous structures[9, 10]. Also Computer aided modeling allows scientist to visualize what is physically happening inside the reactor so as to help them grasp more difficult concepts such as mass transfer. Part of the purpose of this paper is to simulate the oxidation of carbon monoxide over surface of active catalyst using COMSOL Multiphysics.

2. EXPERIMENTAL

2.1. Catalyst preparation

The composite oxides were prepared using co-precipitation methods with slow rate of precipitation. Dilute aqueous solutions containing the desired molar ratios AgNO$_3$, mixed with the

$Fe(NO_3)_3 6H_2O$, solution in the presence of polyethylene glycol. The resulting solution was added drop wise to 60 ml of 0.1N Na_2CO_3 solution at room temperature with vigorous stirring until a solution of pH = 8 was attained. The resulting solution was then placed in a conventional microwave .The microwave power was set to 40% of 650W and operated in 30-s cycles(on for 15s,off for 15s) for 15min and then filtered and washed with distilled water several times for removing excess ions then the composite oxides dried under vacuum.

2.2. Catalyst characterization

The X-ray diffraction (XRD) patterns of the powder samples were measured at room temperature with an X'Pert Philips Materials Research Diffractometer, with CuKα radiation (0.15418 nm, 45kV and 40 mA). The samples were mounted on a silicon plate for X-ray measurements.

Transmission electron microscopy (TEM), the size and morphology of the investigated systems were characterized using a Joel JEM-1230 electron microscope operated at 120 kV. For The TEM imaging, the sample powder dispersed in Methanol by using ultrasonic radiation for 10 minutes and a drop of the suspension was placed onto the carbon-coated grids.

2.3. Catalytic activity measurements

For the CO catalytic oxidation, experiments were carried out by using a quartz flow tube reactor (length 50 cm, i.d. 0.9 cm). 10 mg of the prepared nano catalyst was placed in the middle of the flow tube sandwiched by two pieces of quartz wool, then sandwiched by the other two clean pieces of quartz wool. The quartz flow tube was then placed inside a Thermolyne 2100 programmable tube furnace reactor. The sample temperature was monitored by a thermocouple inserted into the dusted quartz wool. Another thermocouple was placed in the middle of the furnace, outside the flow tube, to monitor and record the furnace temperature. The temperature data were recorded by a Labview-based program. In a typical experiment, 4 wt % CO and 20 wt % O_2 in He was passed over the sample while the temperature was ramped. The gas mixture was set to flow over the sample at a rate of 100 cm^3/min controlled via MKS digital flow meters. The conversion of CO to CO_2 was monitored using an infrared gas analyzer (ACS, Automated Custom Systems, Inc.). All the catalytic activities were measured after a heat treatment of the catalyst at 300 °C in the reactant gas mixture for 15 min in order to remove moisture and adsorbed impurities.

3. RESULT AND DISCUSSION

3.1. XRD investigation of various systems

XRD was used both to identify the phases present in our catalysts and to obtain approximate crystallite size information. Figure 1 depicts the diffractograms of catalysts with different Ag/Fe-Oxide

ratios. It is seen from this figure that: (i) The mixed solids consisted of Ag and AgFeO$_2$ phases. (ii) The positions and relative intensities of Ag-Iron Oxide diffraction peaks matched with standard AgFeO2 at 2θ=28.7°, 32.2°, 33.8°, and 34.8°. (iii) The relative intensity of the diffraction lines of Ag phases increases by increasing the amount of Ag added, and also as a result of Temperature effect. An estimate of particle sizes from the peak width of the peaks reflection using Scherrer's equation is given in Table 1.
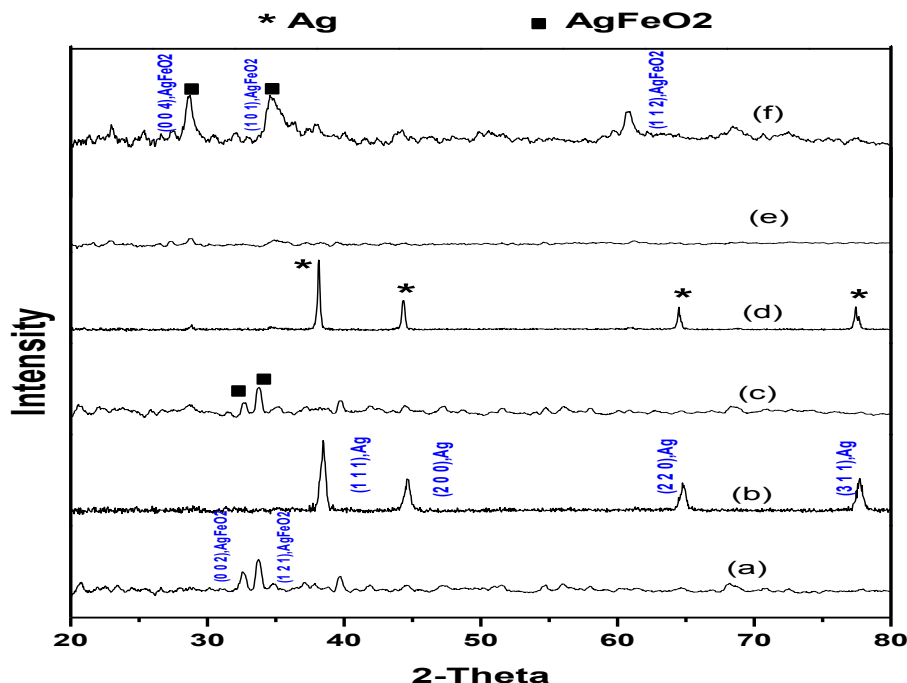

Figure 1. X-ray diffraction powder patterns of Silver: Iron-oxide, (a) (1:1) ratio before,(b) (1:1) ratio After, (c) (1: 0.5) ratio before, (d) (1: 0.5) ratio After, (e) (0.5 :1) ratio before, (f) (0.5 :1) ratio After.

Table 1. Particle size of Ag nano particles before and after catalysis as calculated from Scherrer's equation

Sample		Silver Particle size using Scherrer's equation	
		Before	After
Ag : Fe	**(1:1)**	------	20
Ag : Fe	**(0.5:1)**	------	6
Ag : Fe	**(1:0.5)**	------	44

Empty cells is for particle size which we were not able to calculate, since Xrd's pattern in which metallic Ag nanocrystals were never observed in any of our "as prepared" specimens, which suggests that the Ag is either atomically dispersed, or else is in a sub-nanometer particle

3.2. CO oxidation

In Figure 2, the CO conversion as a function of the temperature is displayed for Ag/Fe-Oxide for the differently prepared samples. In Table 2, the temperatures in correspondence of the 100% conversion are listed. As indicated, the prepared nano catalyst has a remarkable CO oxidation activity; however, its effect is strongly dependent on the preparation ratio between Ag and Fe-Oxide, with the largest activity exhibited by (1:1) ratio since the percentage CO conversion reached 100% at 165 °C with a 50% conversion at 118 °C followed by the (1:0.5) ratio sample which shows CO conversion reached 90% at 411 °C and with the (0.5:1) sample showing the lowest activity, the percentage CO conversion reached 78% at <510 °C.
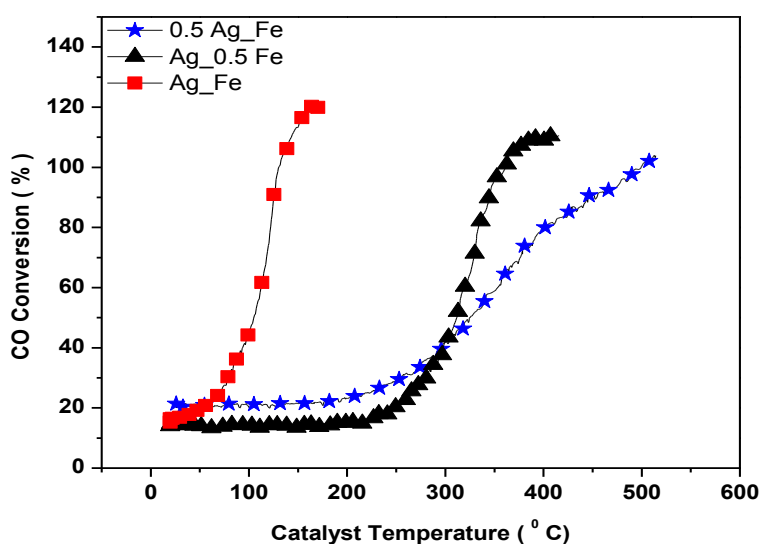

Figure 2. Light off curves of Ag/ Iron-Oxide with different ratios, flow rate: 1000 ml min^{-1}; CO: 4vol.%; O_2: 20 vol.%.

3.3. Transmission electron microscopy

TEM micrographs of the Ag/Fe-Oxide catalysts obtained by Microwave synthesis are shown in Figure 3. nano agglomerates with sizes ranging from 10 to 50 nm were observed. The agglomerates most likely are comprised of amorphous nanoparticles the phase contrast within the agglomerates is characteristic of a disordered or at best semi-crystalline material. It is important to note that Fe-Oxide nanocrystals were rarely observed in any of our "as prepared" specimens either by X-ray diffraction or TEM. This suggests that the oxides is either atomically dispersed, or else is in a sub-nanometer particle form that is impossible to distinguish from the speckle contrast exhibited by the support. but it seems plausible that the silver is homogeneously dispersed, most likely in the form of Ag metal in the prepared catalysts.
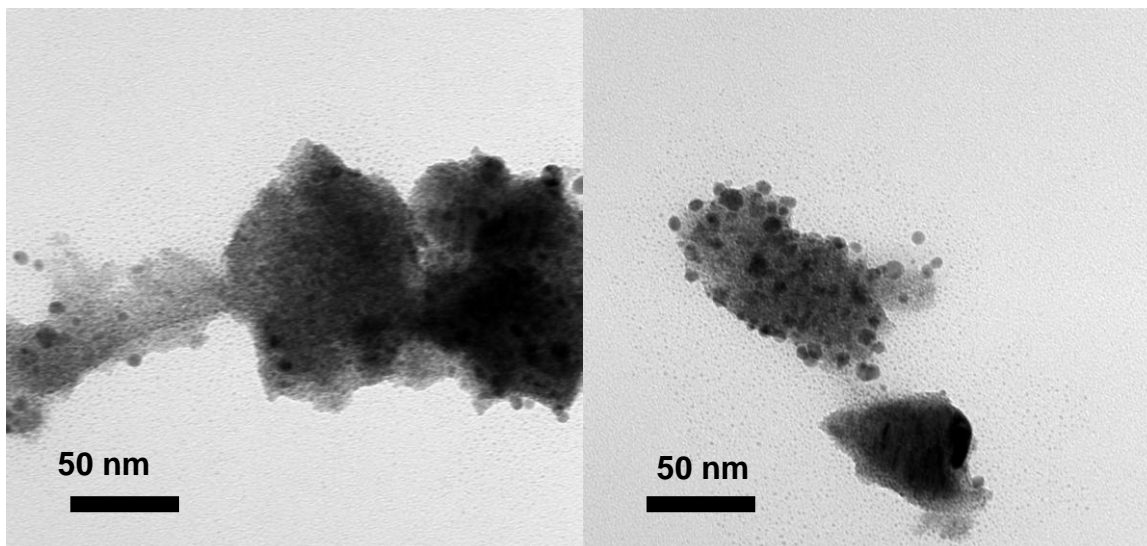
Figure 3. TEM micrographs of Ag/Fe-Oxide obtained by Microwave synthesis.

3.4 Atomistic Modell

The model shows a simple example for surface diffusion and surface reactions coupled to transport of spices to the reacting surface. In most cases you define the reaction rate expression as function of concentration of the reacting species and product. In adsorption reactions however it is also necessary to the surface concentration of active surface are modeled. This implies that the mass balance in the bulk of the reactor must be coupled to the mass balance for species only present at the surface of device. The problem shows of femlab unique features, the coupling of phenomena defined in different geometric dimension. In this case, the model couples the surface process to another defined on volume through femlab extended multi physics features.
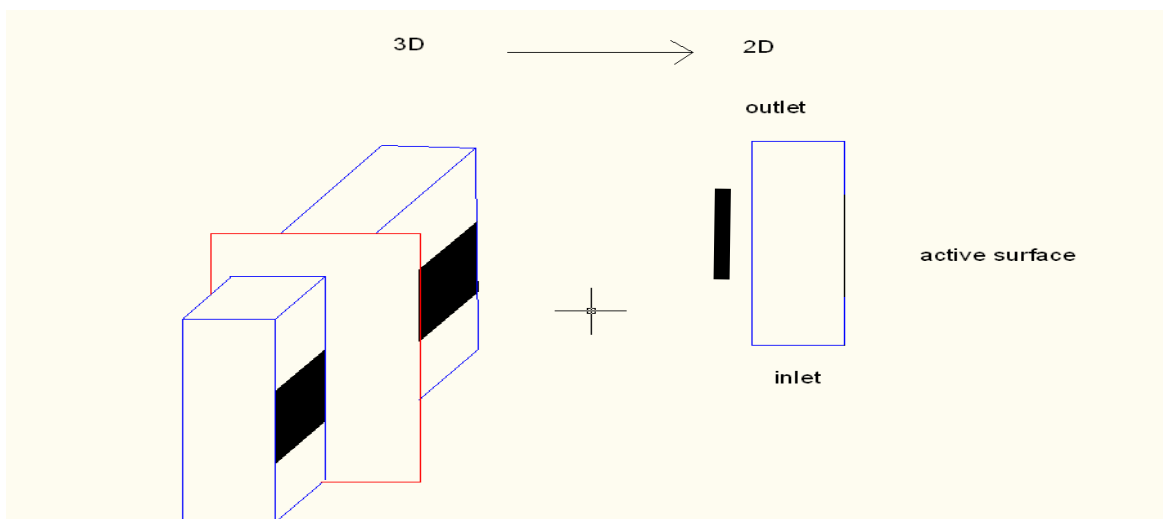

Figure 4. Sketch diagram of reduction the 3D geometry to 2D approximation.

It can be approximated that we can make reduction the 3D geometry to 2D approximation, which is reasonable if the variations in concentration are similar along the sphere.

3.5 Mathematical model

The reaction on the surface of the active surface is given as:

$$K_{ads}C + \theta \Leftrightarrow C_s K_{des} \tag{1}$$

Where:

C: is the bulk concentration.

θ: is the surface concentration of active sites.

C_s: is the surface concentration of adsorbed species.

K_{ads}: is the rate constant for the forward reaction.

K_{des}: is the rate constant for the backward reaction.

The material balance for the surface, including surface diffusion and reaction rate expression for the formation of the adsorbed species C_s is:

$$\frac{\partial C_s}{\partial t} + \nabla.(-D_s \nabla C_s) = K_{ads}C\theta - K_{des}C_s \tag{2}$$

Where:

D_s : represent surface diffusivity.

The equation of reaction rate:

$$\frac{\partial C_s}{\partial t} + \nabla.(-D_s \nabla C_s) = K_{ads}C(\theta_o - C_s) - K_{des}C_s \tag{3}$$

Where:

θ_o: represents the total number of active site available on the surface of drug capsulation.

The initial condition is that the concentration of adsorbed species is zero at the beginning of process:

$$C_s = 0 \tag{4}$$

The transport of drug material in the bulk is described by convection-diffusion equation:

$$\frac{\partial C}{\partial t} + \nabla.(-D\nabla C + Cu) = 0 \tag{5}$$

The initial condition sets the concentration in the bulk at t=0:

$$C = C_o. \tag{6}$$

In above equation:

D: denotes the diffusivity of the reacting species.

C: is its concentration.

u: is the velocity vector.

$$u = (0, V_{max}[1 - (\frac{(x - 0.5\delta)}{0.5\upsilon})^2]) \ . \tag{7}$$

Here:

δ : is the distance between the center of capsulation and the surface.

V_{max} : is the maximum local velocity.

Boundary conditions:

$$n.(-D_s \nabla C_s) = 0 \quad \text{(Insulation condition)} \tag{8}$$

$$n.(-D\nabla C + Cu) = -K_{ads} C(\theta_o - C_s) + K_{des} C_s \tag{9}$$

The other boundary conditions for the bulk problem:

Inlet: $C = C_o$.

Outlet: $n.(-D\nabla C + Cu) = n.Cu \tag{10}$

Insulation: $n.(-D\nabla C + Cu) = 0 \tag{11}$

3.6 Model Results

The concentration, c, in the 2D subdomain after 2 seconds of operation is shown in figure 5. The reaction is very fast and almost reaches steady-state in that time frame.

The cross-section plot demonstrates that the concentration distribution of the reacting species on the surface exhibits end effects on both edges of the catalyst. The edge effect at the lower edge is easy to explain because it is the position closest to the inlet and continuously supplied with fresh reactant. The increase in concentration at the edge at the edge closer to the outlet is due to radial diffusion.
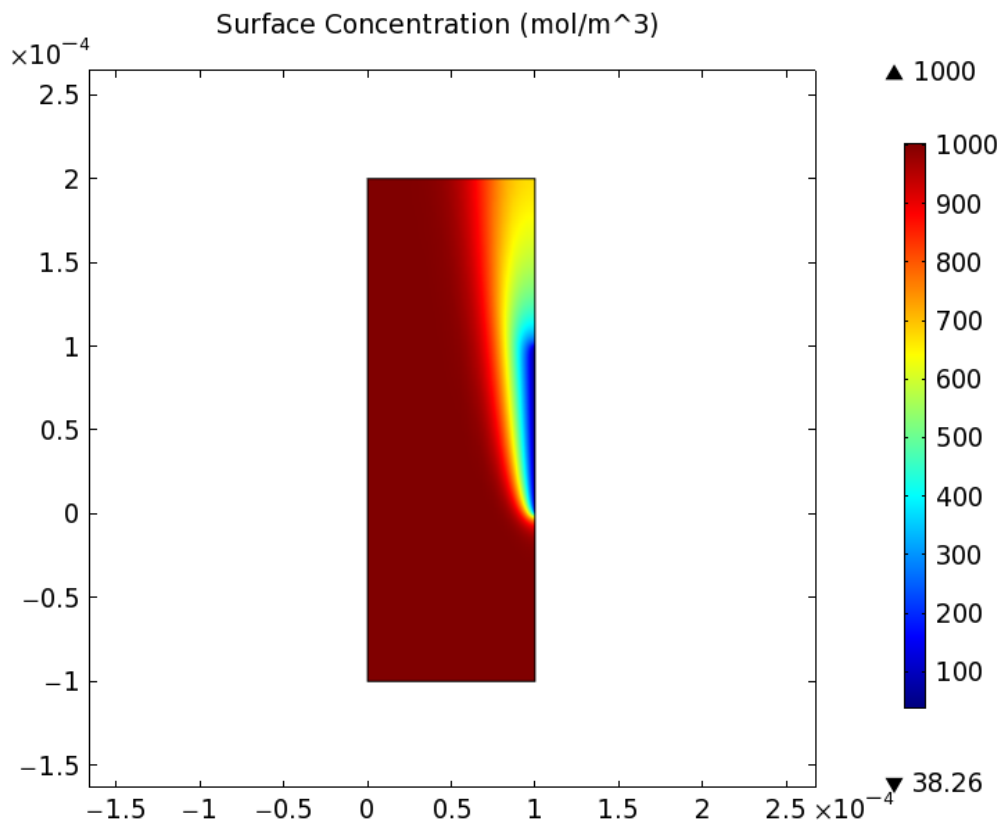
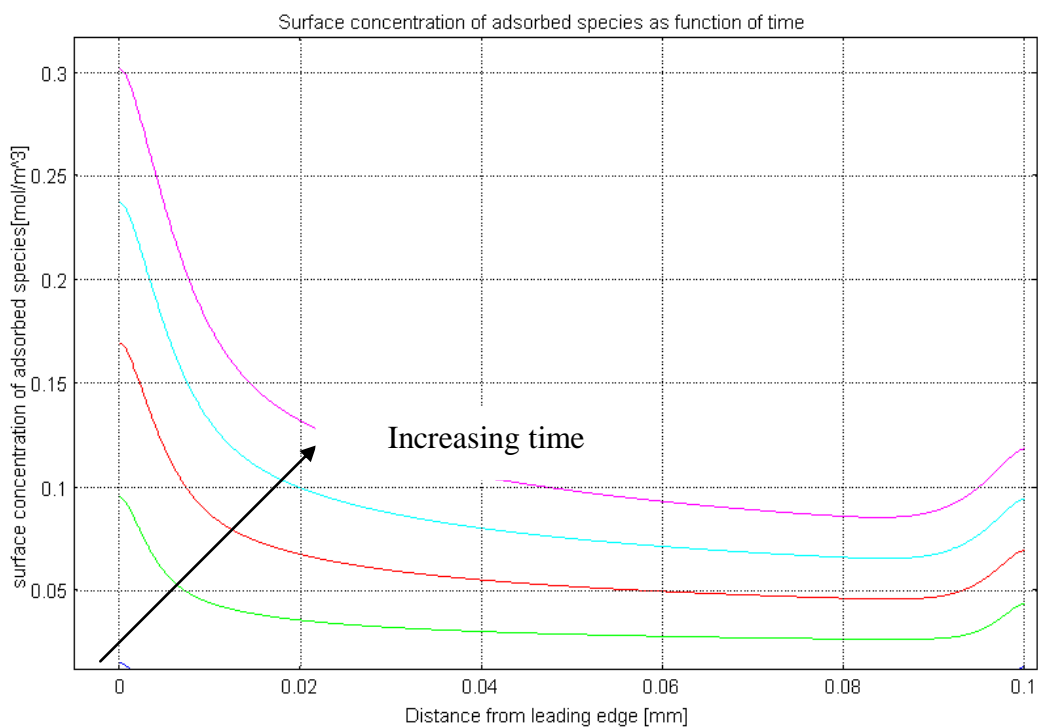**Figure 5.** The concentration of the reacting species, c, after 2 seconds of   operation

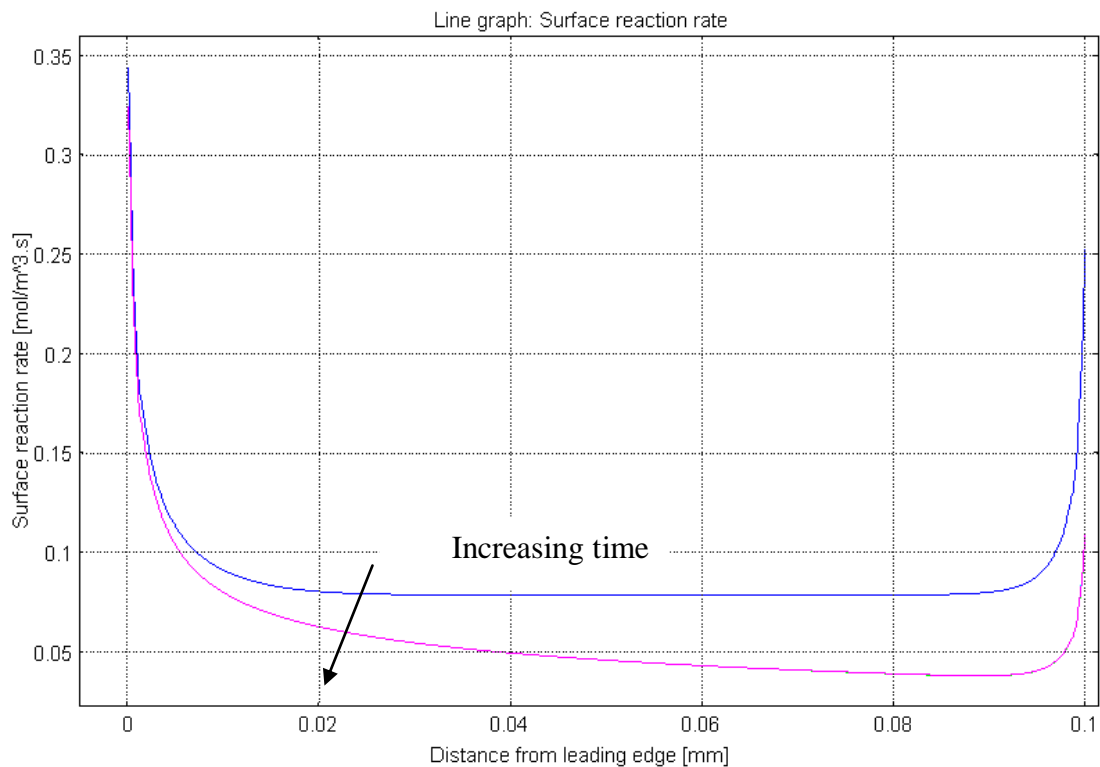**Figure 6.** The concentration of adsorbed species increases with time.

Figure 7. Surface reaction rate at the active surface

Figure 6 shows the concentration of adsorbed species, c_s, illustrates a similar spatial distribution. However, while the concentration of the CO and O2 as reactants decrease with time, the concentration of CO2 as a product species increases. We can also notice that the slight spatial diffusion events out the concentration gradients somewhat. In fig.2 the concentration is plotted after 0.05, 0.5, 1.0, 1.5 and 2.0 second.

Figure 7 illustrates the surface reaction rate decreases with time. As shown after 0.5 s the reaction rate almost reaches steady state. The largest reaction rate is obtained initially and is at the edges of the active surface.

4. CONCLUSION

Ag/Fe-Oxide with different ratios were synthesized through co-precepitation using microwave synthesis method. The prepared nano catalysts were used as CO oxidation catalysts in an attempt to gain insight into how the crystal phase and surface structure influence the oxidation reaction; the prepared catalyst shows a uniform dispersion of Ag nanoparticles with a narrow size distribution within the different oxdies. Also numerical has been developed to show a simple example for surface diffusion and surface reactions coupled to transport of spices to the reacting surface.

References

1. S. Imamura, H. Sawada, K. Uemura and S. Ishida. *Journal of Catalysis*, 109(1) (1988) 198
2. Steven D. Gardner, Gar B. Hoflund, David R. Schryer, Jacqueline. Schryer, Billy T. Upchurch, Erik J. Kielin. *Langmuir,* 7(10) (1991) 2135
3. K. S. Tanielyan, R.L. Augustine,. *Applied Catalysis, A: General*, 85(1) (1992) 3
4. U. Burgaus, H. Conrad, *Surface Science*, 370(1) (1997) 17
5. Jiqing Wang, Martin Castonguay, J. Deng, Peter McBreen. *Surface Science,* 374(1-3) (1997) 197
6. Jiahe Liang, Zhaoxiang Deng, Xin Jiang, Fuli Li, and Yadong Li.   *Inorganic Chemistry*, 41(14) (2002) 3602
7. Garry Glaspell, Hassan M. A. Hassan, Ahmed Elzatahry, Victor Abdalsayed and M. Samy El-Shall. *Topics in Catalysis, 47(1-2)(2008) 22.
8. *K.Suryakala, KR.Marikkannu, G.Paruthimal Kalaignan∗ and T.Vasudevan. Int. J. Electrochem. Sci.,* 3

    (2008) 136 - 144
9. J. Kosek, F. Štˇepanek, M. Marek, *Advances in Chemical Engineering* 30 (2005)137
10. F. J. Keil,*Chemical Engineering Science* 51 (1996) 1543